microbial biotechnology

Open Access

Special Issue Article

A portable library of phosphate-depletion based synthetic promoters for customable and automata control of gene expression in bacteria

Jesús Torres-Bacete,[1,2] José Luís García[2,3] and Juan Nogales[1,2]

[1]*Department of Systems Biology, Centro Nacional de Biotecnología (CSIC), Madrid, 28049, Spain.*
[2]*Interdisciplinary Platform for Sustainable Plastics towards a Circular Economy-Spanish National Research Council (SusPlast-CSIC), Madrid, Spain.*
[3]*Department of Microbial and Plant Biotechnology, Centro de Investigaciones Biológicas (CIB), Centro Nacional de Biotecnología (CSIC), Madrid, Spain.*

Summary

Industrial biotechnology gene expression systems relay on constitutive promoters compromising cellular growth from the start of the bioprocess, or on inducible devices, which require manual addition of cognate inducers. To overcome this shortcoming, we engineered an automata regulatory system based on cell-stress mechanisms. Specifically, we engineered a synthetic and highly portable phosphate-depletion library of promoters inspired by bacterial PHO starvation system (Pliar promoters). Furthermore, we fully characterized 10 synthetic promoters within the background of two well-known bacterial workhorses such as *E. coli* W and *P. putida* KT2440. The promoters displayed an interesting host-dependent performance and a wide strength spectrum ranging from 0.4- to 1.3-fold when compared to the wild-type phosphatase alkaline promoter (P*phoA*). By comparing with available gene expression systems, we proved the suitability of this new library for the automata and effective decoupling of growth from production in *P. putida*. Growth phase-dependent expression of these promoters could therefore be activated by fine tuning the initial concentration of phosphate in the medium. Finally, the Pliar library was implemented in the SEVA platform in a ready-to-use mode allowing its broad use by the scientific community.

Introduction

Microbial growth generally hampers biotechnology objectives because it consumes resources that cease to be available for production processes. Decoupling microbial growth from production processes is seen by many as an optimal solution because it would enable temporary resource allocation, thus avoiding interferences between cell growth and production (Durante-Rodriguez *et al.*, 2018; Stargardt *et al.*, 2020). Fine control of biotechnological output(s) during the initial growth phase maximizes cell biomass by reducing metabolic burdens, while timely expression of biotechnological pathways in a subsequent phase will optimize production (Lo *et al.*, 2016; Lemmerer *et al.*, 2019). Growth-decoupling processes require highly regulated systems, often involving the addition of an inducer or repressor molecule to initiate the expression of the genes responsible for synthesizing the product of interest (Palomares *et al.*, 2004). However, in many cases such inductors usually have a high cost and can become toxic, so post-treatment processes are required to remove them from both the final product and the waste (Menart *et al.*, 2003; Nevoigt *et al.*, 2007). The use of stress inducible promoters to control processes has emerged as an interesting solution to such problems (Hicks *et al.*, 2020). The use of this type of promoter allows the engineering of transcription factor (TF)-based systems capable of detecting environmental changes that trigger gene expression once the cells have reached a desirable growth. Examples of stress-induced promoters include those controlled by temperature (Qing *et al.*, 2004; Yin *et al.*, 2007; Valdez-Cruz *et al.*, 2010) changes in nutrient concentration (Sanders *et al.*, 1998; von der Heyde *et al.*, 2015) heavy metals (Blasi *et al.*, 2012) and quorum sensing (Soma and Hanai, 2015). However, these systems are not free from important drawbacks. In the case of quorum sensing-based

Received 14 December, 2020; accepted 14 March, 2021.
*For correspondence. E-mail j.nogales@csic.es; Tel. +34 915854557; Fax +34 915854506.
Microbial Biotechnology (2021) **14**(6), 2643–2658
doi:10.1111/1751-7915.13808

systems, the difficulty of adjusting cell densities can reduce the system's accuracy (Soma and Hanai, 2015), while systems based on carbon source starvation require adding extra glucose to complete the production process, albeit at reduced yields (Bothfeld *et al*., 2017). Heat-shock inducible promoters face challenging upscaling processes (Caspeta *et al*., 2009), whereas heavy metal-based inducible systems often trigger demanding metabolic responses impacting yield (Blasi *et al*., 2012; Bothfeld *et al*., 2017). However, stress inducible promoters allow less complex decoupling of growth from production cycles in fermentation processes (Lo *et al*., 2016). This advantage facilitates coordination when constrictive synthesis stages are required, delaying the appearance of toxic metabolites and reducing the occurrence of futile cycles that decrease productivity (Engstrom and Pfleger, 2017; Kent and Dixon, 2019). Therefore, the search and development of easily scalable and metabolically harmless portable promoters capable of fine tuning gene expression in a wide range of systems has become an issue of great importance.

Inorganic phosphorus (Pi) is one of the most essential elements in living systems and a key player in their bioprocesses. Pi plays a role as a structural element in DNA, proteins, phospholipids, etc. and as an essential element in the energy metabolism (Santos-Beneit, 2015). *Escherichia coli* uses two different mechanisms to transport Pi into the cell depending on extracellular concentration: (i) a low-affinity Pi transport system (Pit) that operates when there are no extracellular Pi restrictions; and (ii) a specific Pi transport system (Pst). Pst is part of the PHO Pi-starvation system, a global regulatory two-component system involved in phosphate transport and assimilation that comprises over 30 genes in *E. coli* (Gao and Stock, 2013; Uluseker *et al*., 2019). The PHO Pi-starvation system is induced under extracellular Pi depletion and has been extensively studied in *E. coli* (Van Dien and Keasling, 1998). The PHO regulon is finely regulated by the PhoB/PhoR two-component system. The response regulator PhoB is phosphorylated by the histidine kinase PhoR under Pi depletion. Subsequently, the phosphorylated PhoB (PhoB-P) activates transcription of a large set of genes by binding to a conserved operator region, the PHO box, and recruiting the RNA polymerase's subunit σ^{70}. The PHO regulon is widely distributed in bacteria (Hsieh and Wanner, 2010; Santos-Beneit, 2015). Orthologous PhoB have been described in almost 400 different bacterial species belonging to a wide range of phyla, including Proteobacteria, Actinomycetes, Firmicutes and Bacteroidetes (Fig. 1). This wide distribution opens the possibility of developing a set of highly portable promoters regulated by Pi availability in order to control gene expression in bacteria. In fact, the promoter controlling the expression of the phosphatase alkaline (P*phoA*), one of the best characterized PhoB-regulated promoters in *E. coli*, has often been used to develop both phosphate biosensors and gene expression systems (Kikuchi *et al*., 1981). For instance, P*phoA* was used to construct a luminescent biosensor for phosphate detection in wastewater (Dollard and Billard, 2003). The biosensor was further implemented in *E. coli* but also in *Pseudomonas fluorescens*, thus anticipating the portability of this expression system. P*phoA* has been also used to regulate the expression of eukaryotic proteins such as trypsin, interferon alpha and human growth hormone, among others (Miyake *et al*., 1985, Vasquez *et al*., 1989; Gao and Stock, 2015). In this context, the bacterial PHO Pi-starvation regulatory system emerges as a strong candidate for the design and construction of new-to-nature promoters capable of being activated under Pi depletion and triggering the expression of genes of interest in a cost-effective and controlled manner.

In this work, we first construct and analyse a library of Pi depletion synthetic promoters based on the PHO Pi-starvation regulatory system (Pliar promoters). Subsequently, we exploit the potential of synthetic promoters for decoupling growth and expression by developing a tunable and completely self-driven, two-stage bioprocess in *P. putida*. The new promoter library has been implemented in the standardized pSEVA platform for its use worldwide.

Results and discussion

Construction and analysis of a PphoA expression system and its validation in E. coli *W and* P. putida *KT2440*

In *E. coli* the basic structure of P*phoA* includes a PHO box located around the −35 box (5'-CTGTCA-TAAAGTTGTCAC-3'). By taking advantage of its well-known promoter structure, we constructed a P*phoA*-based Pi depletion expression system. The device comprised the P*phoA* promoter and the *msfgfp* gene (GFP) translated by a strong bicistronic RBS (BCD2) as the reporter module (Mutalik *et al*., 2013) (Fig. 2A). As might be expected when using the *E. coli* DH10B strain as a host, P*phoA* showed maximum activity at limited phosphate concentration (< 50 μM), while no activity was registered at higher levels of Pi (≥ 1 mM) (Fig. 2A).

Most traditional studies involving design and characterization of synthetic promoters use laboratory-derived strains, which accumulate growth and functionality-limiting mutations under real-life biotechnological conditions. In order to assess our device with relevant bacterial workhorses, we decided to monitor the performance of P*phoA* in *E. coli* W and *P. putida* KT2440. *E. coli* W (ATCC 9637) has properties that make it a highly

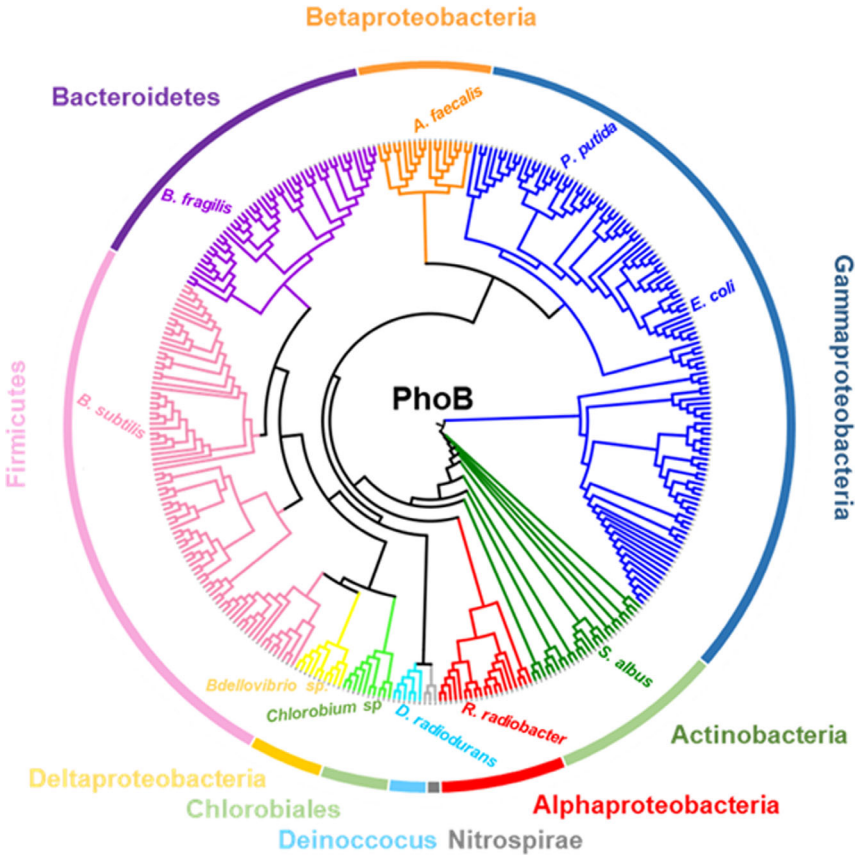

Fig. 1. Phylogenetic tree generated for more than 400 different PhoB protein sequences using *E. coli*'s PhoB protein as a template. Bacteria classes are highlighted in different colours. The phylogenetic tree was constructed using iTOL v5.6.3 (https://itol.embl.de/about.cgi) (Ciccarelli *et al*., 2006).

preferred strain for industrial applications: (i) it produces low amounts of acetate, (ii) it can be grown to high-cell density during fed-batch culture, (iii) it exhibits good tolerance to environmental stresses, and (iv) it is a very fast growing strain with superior growth rate compared to classical K-12-derived strains (Archer *et al*., 2011; Park *et al*., 2011; Felpeto-Santero *et al*., 2015). On the other hand, *P. putida* is a soil bacterium whose value as a workhorse for industrial applications has recently drawn the attention of many authors, mostly due to its high robustness against environmental stress and its capacity to degrade a large array of natural and xenobiotic chemicals and pollutants (Nikel and Lorenzo, 2018; Poblete-Castro *et al*., 2012).

As expected, P*phoA* was also active in *E. coli* W and *P. putida* KT2440 at limited Pi conditions. However, slight host-dependent differences were found: P*phoA* activation required less incubation time in *E. coli* (0.5 vs. 1.5 h), while reduced basal activity (promoter leaking) and higher absolute activity (up to 1.5 times higher) were recorded for *P. puti*da (Fig. 2B, Fig. S1A, B). As previously reported for other PHO-related promoters (Gao and Stock, 2018) the activity of P*phoA* as a function of external Pi followed an inhibitory Hill's function (Eq. 1, Fig. 2C). Using this function, we further estimated several functional parameters of P*phoA,* including basal and maximum activities, the operational (OR) and dynamic (DR) ranges, IC_{50} (Pi concentration supporting 50% of maximum activity), and its Hill´s constant (K), which is dependent on the binding cooperativity between TF PhoB-P and the PHO box (Fig. 2D) (Ang *et al*., 2013).

P*phoA* activity in *E. coli* W showed higher activity at Pi concentrations below 0.1 mM, peaking at concentrations ranging from 0 to 50 μM. This is in good agreement with previous reports (Lübke *et al*., 1995). P*phoA* activity significantly decreased at higher concentrations and was completely repressed at concentrations above 0.2 mM (Fig. 2C). The estimated OR value was 0.2 mM for IC_{50} 0.12 mM, while DR showed an 11-fold activity increase for the promoter. The value of Hill´s constant was 2, which is within the range of K values calculated elsewhere for the *phoB* (1.9) (Ritzefeld *et al*., 2013) and *phoA* (1.6) (Gao and Stock, 2015) promoters. This seems to be related to a TF PhoB-P dimer binding to the promoters' single PHO box (Blanco *et al*., 2012; Gao and Stock, 2018).

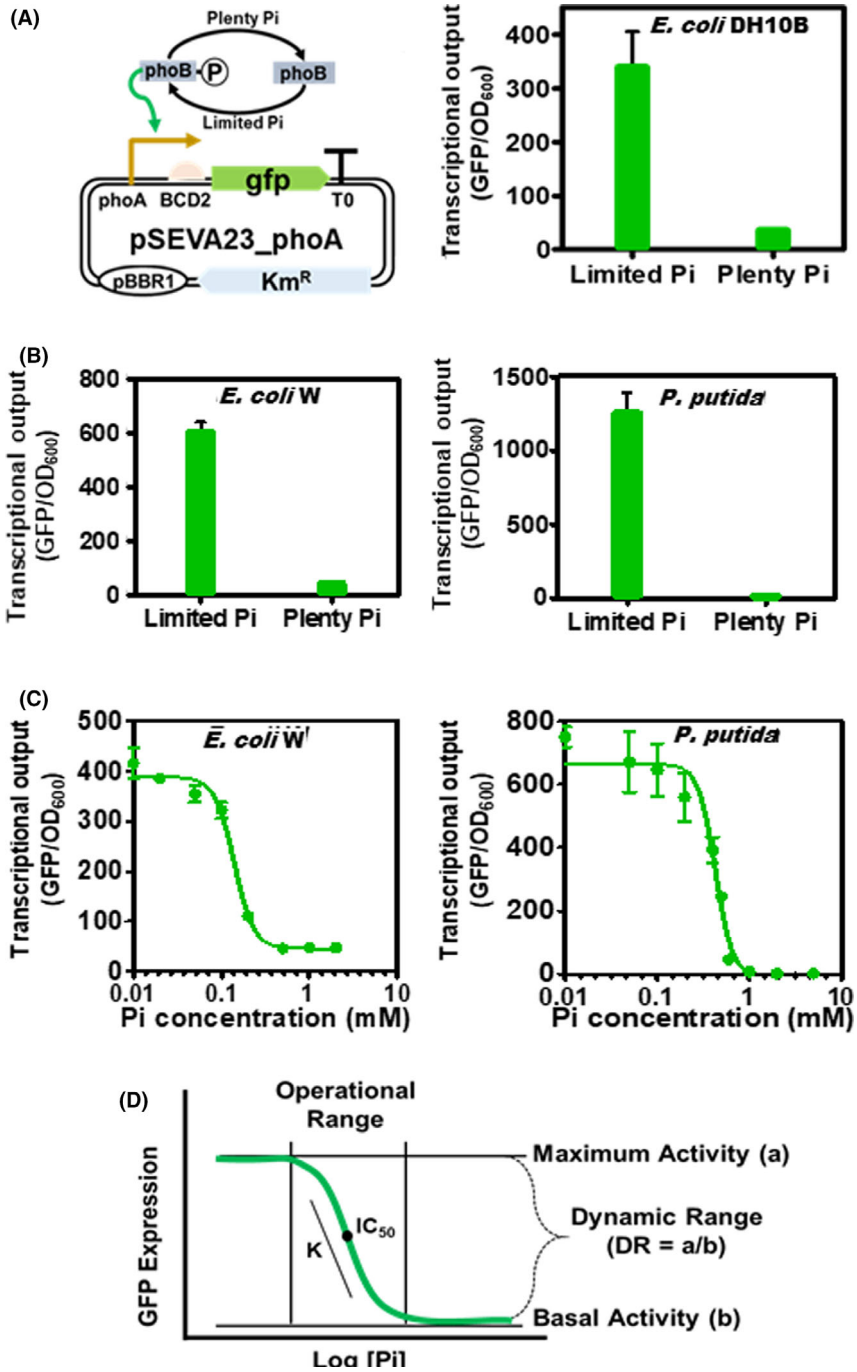

Fig. 2. A. Left, Design of pSEVA23_*phoA*, where the *phoA* promoter (P*phoA*) was fused to the BCD2 bicistronic RBS and the reporter *msfgfp* gene. P*phoA* is activated by the binding of a dimer of the phosphorylated transcription factor PhoB (PhoB-P); Right, GFP fluorescence response of *E. coli* DH10B under the control of P*phoA* at limited (50 μM) and plenty (1 mM) Phosphate (Pi).
B. GFP fluorescence response of *E. coli* W (left) and *P. putida* KT2440 (right) under the control of P*phoA* at limited and plenty Pi.
C. Experimental dose–response curves of the P*phoA* in *E. coli* W (left) and *P. putida* KT2440 (right).
D. Sigmoidal dose–response curve or Hill´s function used to calculate the activity parameters of P*phoA* and the Pliar promoters. P*phoA* activity was measured as GFP expression in MOPS minimal medium with 0.2% glucose supplemented with phosphate at 37 C for *E. coli* and at 30 C for *P. putida*.

The behaviour of P*phoA* in *P. putida* KT2440 showed interesting differences when compared with *E. coli* W (Fig. 2C). The promoter retained peak activity at phosphate concentrations that doubled those for *E. coli* (0.1 mM). In addition, P*phoA* remained active at Pi concentrations as high as 0.6 mM, which resulted in a

threefold increase in OR and a higher IC_{50} value (0.43 vs. 0.12 mM). P*phoA* also displayed higher DR and *K* values in *P. putida* (10 and 2 times higher, respectively). The calculated *K* value was also over twice as high in *P. putida* than in *E. coli* W. This steeper sensitivity could be due to an increase in cooperative binding of TF PhoB-P to the PHO box or to the existence of a cellular process that increases sensitivity (Ang *et al*., 2013).

Despite observed host-dependent differences in behaviour, we proved the potential of P*phoA* (and likely other P*phoA*-based promoters) as suitable gene expression systems for different biotechnological bacterial workhorses. These results and the inferred broad universality of the PHO two-component system (Fig. 1) pave the way for the construction of highly portable gene expression systems in bacteria. In order to generate tools to support optimization and tight regulation of biotechnological processes based on the PHO Pi-starvation system, we generated a set of new-to-the-nature synthetic promoters to expand the spectrum of promoter activity strengths.

Combinatorial construction and screening of a library of synthetic Pi-dependent promoters (Pliar)

Common strategies used to engineer synthetic promoters entail: (i) random and site directed mutagenesis of natural promoters by using error-prone DNA polymerases and/or degenerated (randomized) oligonucleotides, and (ii) the construction of hybrid promoters combining structural parts of different promoters to obtain the desired functionality (Johnson *et al*., 2018; Yang *et al*., 2018). To engineer synthetic Pi-starvation promoters we used a combined strategy, where sequence-randomized PHO boxes were introduced in the −35 box of a strong constitutive promoter (BG42) (Zobel *et al*., 2015). The overall workflow is shown in Fig. 3. In order to design a fully portable synthetic PHO Box, we analysed known PHO boxes from several Gram positive and negative bacteria, thus generating a consensus sequence which included multiple variable positions (Fig. 3A, Fig. S2). The consensus sequence was further used as a template to design a set of degenerate primers, including thousands of alternative PHO Boxes. Using these primers, we amplified the constitutive promoter BG42 to deliver a large library of putative synthetic promoters that included alternative PHO Boxes (Pliar promoters). These synthetic promoters included the −10 region from BG42 and a variable PHO box located around the −35 region (Fig. 3B). To facilitate library screening and the characterization of the new synthetic Pliar promoters, and following the procedure for P*phoA*, they were fused to BCD2 and the reporter gene *msfgfp*, thus generating the pSEVA23_Pliar vectors, Fig. 3C.

The initial screening step was performed directly using the cloning strain *E. coli* DH10B. After transformation, colonies showing GFP fluorescence only under Pi limitation but not under Pi excess were selected for further analysis. In a second screening step, the GFP fluorescence of positive colonies was quantitatively evaluated in MOPS minimal medium at plenty and limited Pi concentrations. Remarkably, the single inclusion of a −35 box by PHO boxes in the −35 position was enough to become the constitutive BG42 in a Pi-depleting regulated promoter. The inclusion of alternative PHO boxes guided a large distribution of promoter strengths (Fig. 3D), ranging from promoters exhibiting similar activity to that found in P*phoA* at limited Pi concentration, for example Pliar 52 and 53, to promoters displaying weak promoter activities (Pliar 15, 3, 56) and even stronger activity (Pliar 51). With plenty Pi, similar to P*phoA*, most of the Pliar promoters showed reduced activity. However, several promoters retained elevated basal activity, for example Pliar 51 and 68. From this first set of analysed promoters, we selected ten covering the full spectrum of activity strengths for further studies and characterization with relevant industrial strains such as *E. coli* W and *P. putida* KT2440. The selected synthetic Pliar promoters were: 1, 10, 15, 17, 51, 52, 53, 59, 68 and 70 (Fig. 3D).

Activity and performance of Pliar synthetic promoters in E. coli *W*

The selected Pliar promoters were transferred to *E. coli* W and their behaviour monitored as a function of the Pi concentration (Fig. 4A). All of them showed peak activity in the absence of extracellular phosphate, (Fig. 4A, Fig. S3). Similar to P*phoA*, at extracellular Pi concentrations higher than 0.2 mM all of them were repressed, showing only basal activity. The broad variability of basal activities displayed by the different Pliar promoters is quite remarkable. The strongest (Pliar 51, 59 and 68) were also those displaying the highest basal activities (up to 5 times higher than in P*phoA*). On the contrary, the weakest promoters (Pliar 1, 15 and 10) had lower basal activity at high-Pi concentrations (over 5 times lower than P*phoA*). The data from the dose–response curve was subsequently adjusted to Hill's function (Fig. 4 B, Fig. S4). Despite the wide range of activity strengths displayed by the Pliar promoters, it should be noted that all of them had OR (~ 0.2 mM) IC_{50} (~ 0.12 mM) and K (~ 2) values similar to those estimated for the wild-type P*phoA*. In fact, most of the variability observed was due to differences in their basal and peak activities, which promoted a broad spectrum of DRs. It would thus be reasonable to think that the nucleotide sequence of the synthetic promoters determines their strength. In fact, we noted that the weakest promoters were those with the

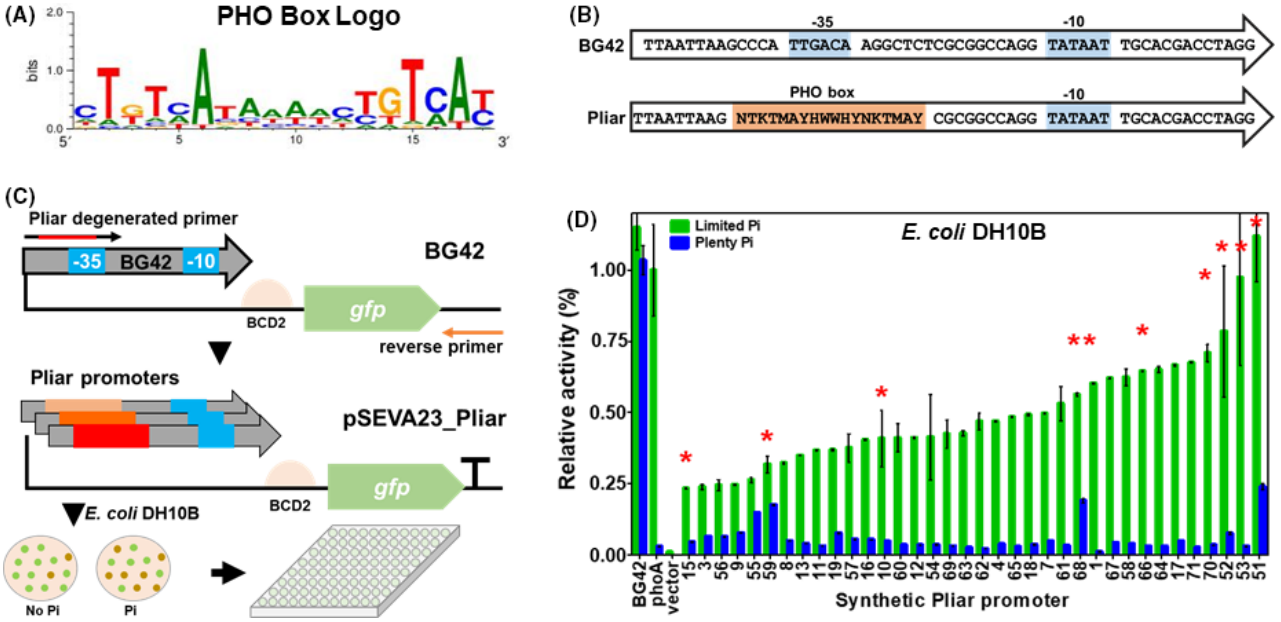

Fig. 3. A. Sequence Logo of the PHO box. The consensus sequence was constructed using WebLogo3 (Schneider and Stephens, 1990; Crooks *et al.*, 2004).
B. Diagrams and sequences of the BG42 and Pliar promoters.
C. Schematic representation showing the construction of the Pliar promoters using degenerated primers and the BG42 promoter as a template and pSEVA23_Pliar vectors. The diagram also shows the GFP fluorescence high-throughput screening used to select positive Pliar promoters.
D. Screening for active Pliar Pi-starvation promoters in MOPS minimal medium using *E. coli* DH10B cells at limited and plenty extracellular Pi concentration. The asterisks indicate selected Pliar promoters.

highest percentage of GC in the PHO box (Fig. 4B). This effect has been previously described for variants of the Plac promoter in *E. coli*. Authors analysed different spacer sequences between the −35 and −10 regions and it seemed that higher GC percentages increased the resistance to separate DNA strands (Liu *et al.*, 2004). However, some exceptions were found, for example Pliar 70, which has a low-GC content (17%) and still exhibits medium-strength activity similar to that of P*phoA*.

Overall, based on the estimated functional parameters, the synthetic Pliar promoters could be clustered in four groups using clustergram analysis (Eisen *et al.*, 1998) (Fig. 4B):

i. *PhoA*-Like Promoters: Promoters that showed regulatory activity akin to P*phoA* (Pliar 59, Pliar 53 and Pliar 70).
ii. High-strength Promoters: Promoters with high-activity irrespective of Pi concentrations and showing lower dynamic range (Pliar 51, and 68).
iii. Medium-strength Promoters: Promoters exhibiting medium strength at low Pi and not completely repressed at Pi concentration above 200 μM (Pliar 17 and 52).
iv. Low-strength Promoters: They are the weaker promoters, with peak activity more than two times lower than *PhoA*-like promoters. Interestingly, these were the promoters with higher DR (Pliar 1, 10 and 15).

Activity and performance of Pliar promoters in P. putida *KT2440*

The Pliar library was further analysed in *P. putida* KT2440 and, similar to our findings with *E. coli* W, the promoters displayed a Pi-dependent repression and an extended spectrum of activity (Fig. 5A, Fig. S5). However, notable differences were found. For instance, Pliar promoters had null leaking activity at high-Pi concentrations, which was in contrast to the behaviour exhibited in *E. coli*. Remarkably, Pliar 51, 59 and 68's basal activity was over 10-times lower in *P. putida* and they triggered higher activity than in *E. coli* W (Figs S4 and S6). On the whole, these results argue in favour of a major control of Pliar promoters' gene expression in *P. putida*.

Overall, the synthetic promoters showed significantly larger DR when compared with *E. coli*. Greater OR, around 0.6 mM, were also estimated and they consistently showed higher IC_{50} values (up to 4 times higher for most analysed promoters) (Fig. 5B, Fig. S6). Estimated K values showed wide variability, ranging from 1.5 in Pliar 15 to the steeper slope of 8.1 observed in Pliar 52. These values confirmed the higher sensitivity of

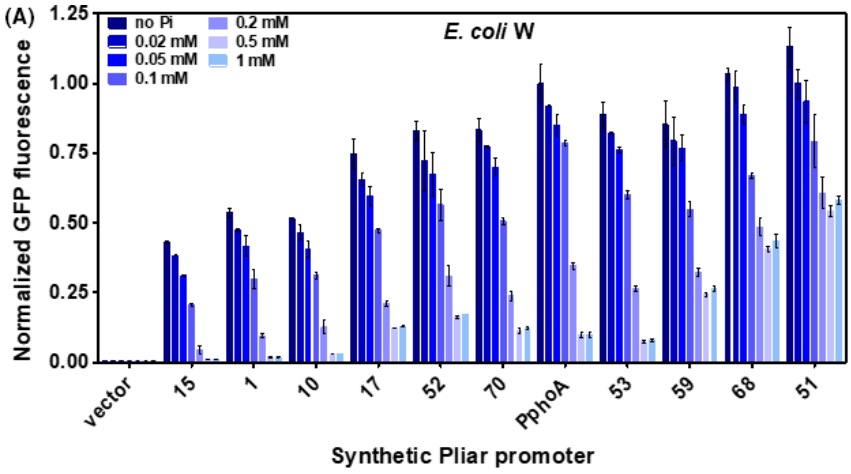

(B)

Promoter	Pho box	IC_{50}[a]	K[b]	Basal activity[c]	Maximum activity[d]	DR[e]	OR[f]	G+C[g]
High-strength Pliar promoters								
Pliar 51	GTGTAATAATATGGTAAC	0.08	-1.7	0.54	1.13	2.1	0.15	28%
Pliar 68	ATGTCATAAAATATTAAC	0.09	-2.3	0.40	1.03	2.5	0.15	17%
PphoA-like Pliar promoters								
Pliar 59	CTGTAATATTCTTTTCAT	0.10	-2.9	0.24	0.85	3.6	0.20	22%
Pliar 53	TTGTCACATATCTGTCAT	0.13	-2.5	0.07	0.88	12.6	0.20	33%
PphoA	CTGTCATAAAGTTGTCAC	0.12	-2.0	0.09	1.00	11.1	0.20	39%
Pliar 70	TTGTCACATTTTTTTAAT	0.10	-2.5	0.11	0.83	7.5	0.20	17%
Medium-strength Pliar promoters								
Pliar 52	CTGTCATTTAATTGTAAC	0.13	-1.8	0.16	0.83	5.2	0.25	28%
Pliar 17	ATGTCATTATATTGTCAC	0.11	-2.3	0.12	0.75	6.2	0.15	28%
Low-strength Pliar promoters								
Pliar 10	CTGTCATTATCCTGTCAC	0.11	-2.0	0.03	0.51	17.0	0.20	44%
Pliar 1	CTGTCACTTTCTGGTAAC	0.10	-2.2	0.02	0.53	26.5	0.15	44%
Pliar 15	GTGTCACTAACCGGTCAT	0.09	-2.1	0.01	0.43	43.0	0.15	50%

Fig. 4. A. Comparison of Pliar promoters' activity in *E. coli* W at increasing Pi concentration. Pliar activity in terms of GFP fluorescence was measured in resting cells and normalized considering P*phoA* activity as the reference (value of 1). Readings were taken after 3.5 h' incubation at 37 C in MOPS minimal medium, 0.2% glucose, supplemented with phosphate.
B. Activity parameters for the synthetic Pliar promoters in *E. coli* W were calculated using Hill´s function, where [a]IC_{50} is half maximal inhibitory concentration, [b]K is Hill´s constant, [c]normalized basal activity, [d]normalized maximum activity, [e]dynamic range, [f]operational range, [g]guanine and cytosine percentage. Promoter clusters were ordered according to their parameters using clustergram analysis.

Pliar promoters in *P. putida*. Therefore, since Pi is necessary for many cellular processes, the extended OR and higher sensitivity observed in *P. putida* opens the possibility of regulating biotechnological processes at a wider range of Pi concentrations than in *E. coli*, thus avoiding extreme conditions of phosphorus stress (Givskov *et al*., 1994). No direct relationship could be established between the nucleotide sequences of PHO boxes and promoters' behaviour. As was done for *E. coli*, they were clustered into four groups according to their performance (Fig. 5B).

i. *PhoA*-Like Promoters: Promoters that showed regulatory activity similar to P*phoA* (Pliar53 and Pliar52).
ii. High-strength Promoter: A Promoter with high activity at low-Pi concentrations, showing the higher dynamic range (Pliar 1).
iii. Medium-strength Promoters: Promoters displaying medium strength at low Pi (Pliar17, 51 and 68).
iv. Low-strength Promoters: Weaker promoters with peak activity more than 2 times lower than *PhoA*-like promoters (Pliar10, 15, 70 and 59).

Interestingly, some promoters displayed a very different behaviour depending on the host: Pliar 1, which was a weak promoter in *E. coli*, becomes the strongest in *P. putida*. On the contrary, while Pliar 70 and 59 showed a P*phoA*-like behaviour in *E. coli,* they displayed low activity in *P. putida*. Overall, these data stress the need for a broad library of promoters in order to cover optimal gene expression requirements for different bacterial hosts.

Poly phosphate accumulation drives the different behaviour of Pliar promoters in P. putida

Due to the essential role that Pi plays in growth, most microorganisms accumulate it in the form of

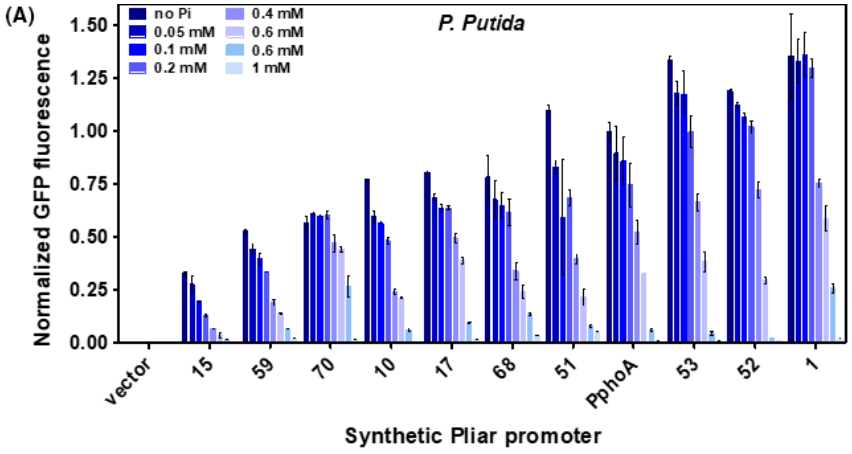

(B)

Promoter	Pho box	IC_{50}[a]	K[b]	Basal activity[c]	Maximum activity[d]	DR[e]	OR[f]	G+C[g]
high-strength Pliar promoters								
Pliar 1	CTGTCACTTTCTGGTAAC	0.44	-3.9	0.01	1.35	135	0.70	44%
PhoA-like Pliar promoters								
Pliar 52	CTGTCATTTAATTGTAAC	0.44	-8.1	0.01	1.20	120	0.60	28%
Pliar 53	TTGTCACATATCTGTCAT	0.41	-4.7	0.01	1.33	133	0.60	33%
PphoA	CTGTCATAAAGTTGTCAC	0.43	-4.7	0.01	1.00	100	0.60	39%
Medium-strength Pliar promoters								
Pliar 51	GTGTAATAATATGGTAAC	0.30	-2.2	0.05	1.10	22	0.60	28%
Pliar 68	ATGTCATAAAATATTAAC	0.38	-2.7	0.03	0.78	26	0.65	17%
Pliar 17	ATGTCATTATATTGTCAC	0.49	-6.1	0.02	0.81	40	0.65	28%
low-strength Pliar promoters								
Pliar 10	CTGTCATTATCCTGTCAC	0.28	-1.7	0.01	0.77	77	0.60	44%
Pliar 70	TTGTCACATTTTTTTAAT	0.58	-5.0	0.02	0.56	28	0.80	17%
Pliar 59	CTGTAATATTCTTTTCAT	0.29	-1.6	0.02	0.53	26	0.60	22%
Pliar 15	GTGTCACTAACCGGTCAT	0.14	-1.5	0.01	0.33	33	0.55	50%

Fig. 5. A. Comparison of the Pliar promoters' activity in *P. putida* KT2440 at increasing Pi concentration. Pliar activity in terms of GFP fluorescence was measured in resting cells and normalized considering P*phoA*'s activity as the reference (value of 1). Readings were taken after 3.5 h' incubation at 30 C in MOPS minimal medium, 0.2% glucose supplemented with phosphate.
B. Activity parameters or the synthetic Pliar promoters in *E. coli* W were calculated using Hill´s function, where [a]IC_{50} is half maximal inhibitory concentration, [b]K is Hill´s constant, [c]normalized basal activity, [d]normalized maximum activity, [e]dynamic range, [f]operational range, [g]guanine and cytosine percentage. Promoter clusters were ordered according to their parameters using clustergram analysis.

polyphosphate (poly-Pi). However, this poly-Pi storage ability is largely species-dependent (Kulakovskaya, 2015). For instance, it is well-known that *E. coli* accumulates poly-Pi to a very low extent (Nesmeyanova, 2000), while *P. putida* has a very active poly-Pi accumulation system that drives Pi accumulation in large quantities throughout their whole life cycle (Nikel *et al.*, 2013). Therefore, differential phosphate accumulation abilities of these two strains could likely be responsible for differences in behaviour exhibited by the PHO-based promoters. In the case of *E. coli*, the concentration of extracellular Pi should remain more stable overtime, thus resulting in repressed promoters at concentrations greater than 0.2 mM. On the contrary, *P. putida*'s higher capacity to accumulate Pi could result in a significant reduction of extracellular Pi, thus leading to promoter activation, even at high initial phosphate concentrations.

To test this hypothesis, we grew both strains in the presence of 2.5 mM phosphate and monitored the amount of Pi in the supernatant over time. In both cultures, we observed a growth-dependent decrease in the levels of Pi. However, while in the case of *E. coli* this was observed only in the exponential phase, in *P. putida* the reduction of Pi extends throughout the complete growth curve (Fig. 6A and B). *E.* coli was only able to reduce the initial Pi concentration by 27%, which is in good agreement with previous reports indicating that *E. coli* only removed extracellular Pi during the exponential growth phase (Lübke *et al.*, 1995). On the other hand, *P. putida* KT2440 was not only able to eliminate almost 50% of the initial phosphate during the exponential growth phase, but it continued to remove Pi in the stationary phase and reduced the concentration by up to 80% after 24 h (Fig. 6B). Therefore, active Pi removal could explain why Pliar promoters displayed activity in *P. putida* even at high-phosphate concentrations. In fact, it is reasonable to think that *P. putida* efficiently reduces the concentration of extracellular Pi to a critical level, thus triggering promoter expression irrespective of the initial Pi concentration in the culture medium.

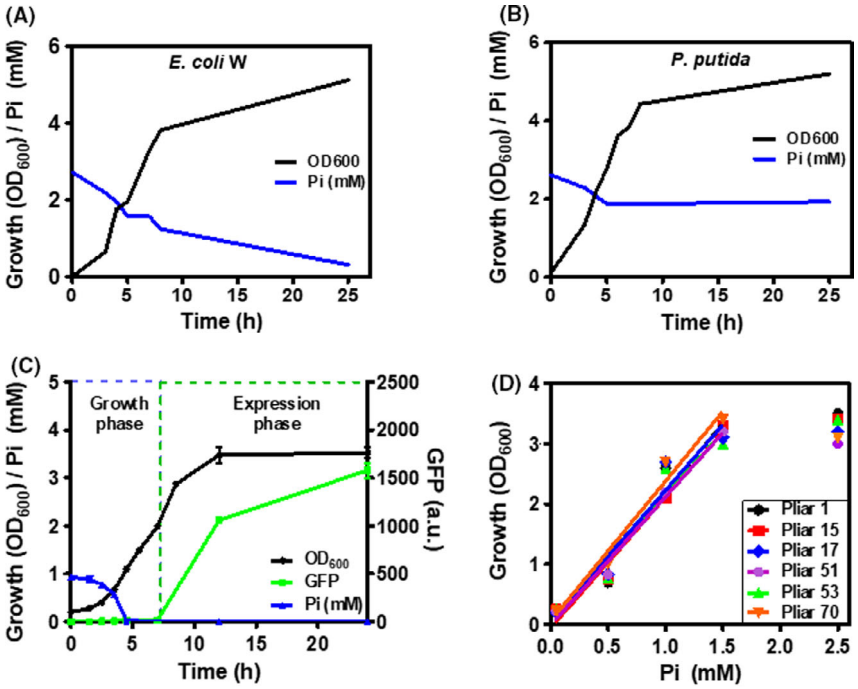

Fig. 6. A. Time course of extracellular Pi consumption coupled to growth of *E. co*li W in LB medium at 37 C.
B. Time course of extracellular Pi consumption coupled to growth of *P. putida* KT2440 in LB medium at 37°C.
C. Time course of growth, extracellular Pi consumption and Pliar 53 activity in *P. putida* KT2440. Pliar 53 activity was measured as fluorescence GFP expression in 50 ml MOPS minimal medium with 0.4% glucose supplemented with 1 mM phosphate in a 250 ml flask at 30 C. For details see Material and Methods.
D. Correlation between the initial extracellular Pi concentration and *P. putida* KT2440 growth (OD_{600}) at which Pliar promoters triggered the expression of GFP. The cultures were initiated at 0.2 OD_{600} in MOPS minimal medium, 0.4% glucose, supplemented with 0.05, 0.5, 1, 1.5 and 2.5 mM Pi at 30 C. The linear regression equations calculated for each promoter are: Pliar 1 : OD_{600} = 2.2Pi(mM) - 0.01 (R^2 = 0.95); Pliar 15 : OD_{600} = 2.1Pi(mM) – 0.05 (R^2 = 0.98); Pliar 17 : OD_{600} = 2.1Pi(mM) + 0.04 (R^2 = 0.93); Pliar 51 : OD_{600} = 2.1Pi(mM) + 0.04 (R^2 = 0.94); Pliar 53 : OD_{600} = 2.1Pi(mM) + 0.06 (R^2 = 0.99); Pliar 70 : OD_{600} = 2.3Pi(mM) + 0.06 (R^2 = 0.97).

A Pliar-based gene expression system for decoupling growth and production in P. putida *KT2440*

The ability of *P. putida* KT2440 to linearly reduce the external Pi concentration along its whole life cycle paves the way for designing a novel growth-decoupled gene expression system based on PHO-related promoters. Furthermore, Pliar promoters could be used to engineer a pre-programed, two-phase, growth-decoupled biotechnological process. In order to address this challenge, we monitored both GFP-based fluorescence and OD600 over time in a culture of *P. putida* harbouring the *msfgfp* gene under the control of Pliar 53, a promoter that showed strong activity and suitable fine control in this strain (Fig. 5). When the cells grew in the presence of 1 mM of Pi, the poly-Pi accumulation abilities of *P. putida* promoted the appearance of two well-defined phases: i) a growth phase in which *P. putida* grew by consuming the available Pi, and ii) an expression phase following Pi depletion (Fig. 6C). During the growth phase, Pi in sufficient amounts promoted the full repression of promoter Pliar 53, thus avoiding undesirable metabolic loads and facilitating optimal resource allocation for robust growth. Following Pi depletion, *P. putida* not only suddenly stopped growing, but the activation of Pliar 53 drove an intense GFP-derived fluorescence that triggered the expression phase.

Since Pi depletion associated to cellular metabolism drives the activation of the PHO promoters, it is reasonable to think that the activation of Pliar promoters could be finely controlled by tuning the level of initial Pi in the culture medium. In other words, using Pliar promoters it would be possible to select the desirable cell biomass responsible for a given biotechnological output in a two-phase, growth-decoupled bioprocess just by adjusting the initial concentration of Pi. This controlled expression could be pre-programmed and would avoid the need for costly downstream processes to remove inducers while supporting self-induction bioprocesses. To test the feasibility of this interesting system, the fluorescence of *P. putida* cells harbouring the *msfgfp* gene under the control of several Pliar promoters was monitored over time in MOPS minimal medium using 0.05, 0.5, 1, 1.5 and 2.5 mM phosphate concentrations (Fig. 6D). In good

agreement with our reasoning, the higher the initial Pi concentration in the medium, the higher bacterial growth was required to activate the synthetic promoters. In fact, at extracellular Pi concentrations of up to 1.5 mM, we observed a linear correlation between initial Pi concentration and cellular biomass (measured as OD_{600}) and the Pliar promoters became active regardless of the promoter analysed (Fig. 6D). At Pi concentrations between 1.5 and 2.5 mM, the Pliar promoters became active once *P. putida* reached its peak growth ($OD_{600} > 3$). Using these linear correlations, the Pliar library became a very effective tool not only for decoupling growth from production but also to control, ad hoc, the biomass required to trigger production according to the needs of the process. For instance, in the case of the production of toxic metabolites, the decoupled bioprocesses could be initiated using high-phosphate concentrations, for example 1.5 mM. In this scenario, the production stage could only start once enough biomass has accumulated ($OD \geq 3$). On the contrary, when just a limited amount of cellular biomass is required, the use of lower initial Pi concentrations might facilitate swift induction of Pliar promoters, thus delivering greater levels of production from the start of the process. In addition, the large range of activities and functional parameters contained in the Pliar library supports a wide choice of optimal promoters based on the requirements of biotechnological processes. In addition, the ability to select suitable promoters from the Pliar library will further expand gene expression-based control of target bioprocesses.

Finally, we contextualized the Pliar library within gene expression systems widely used in *P. putida* by comparing the performance of Pliar 53 promoter with *Xyls/*P_m, *RhaRS/*P_{rhaB} and *lacI*^{q}/P_{trc} (de Lorenzo *et al.*, 1993; Gawin *et al.*, 2017; Jeske and Atenbuchner, 2010). For this, we constructed a series of plasmids expressing the fluorescent reporter RFP under the control of Pliar 53, P_m, P_{rhaB} and P_{trc}, and monitored the RFP-based fluorescence in *P. putida* cells under growing conditions (Fig. 7, Fig. S7). Noteworthy, we found interesting advantages when using the Pliar 53 system including: i) a lower basal activity and higher dynamic range than in the other systems, despite similar maximum activity was monitored and, ii) the decoupling of growth from production using the Pliar 53 had a negligible effect on growth rate (≈ 10% reduction), while higher reduction was found using *RhaRS/*P_{rhaB} (20%) and *Xyls/*P_m (40%). In the case of the *lacI*^{q}/P_{trc} the elevated basal expression displayed affected the bacterial growth, even in absence of inductor (Fig. 7). In addition, it's remarkable the fact that since Pliar system does require adding exogenous inductor, the fermentation cost of a putative bioprocess based on this system would be significantly cheaper than using either *RhaRS/*P_{rhaB}, the *XylS/*P_m or *LacI*^{q}/P_{trc} system.

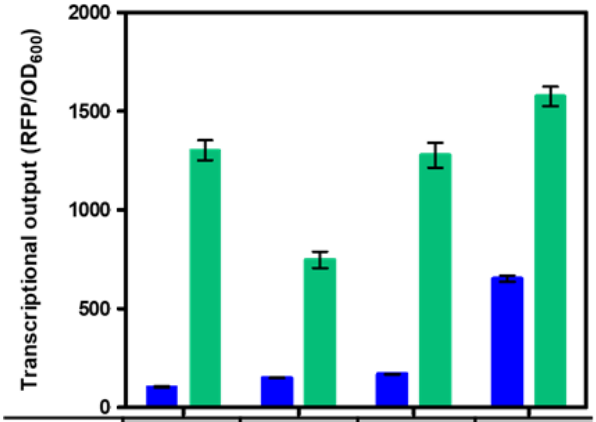

	Pliar 53		*RhaRS/*P_{rhaB}		*XylS/*P_m		*LacI*^{q}/P_{trc}	
Pi[1]	5	0.5	5	5	5	5	5	5
Rhamnose[1]	-	-	-	1	-	-	-	-
m-toluic[1]	-	-	-	-	-	1	-	-
IPTG[1]	-	-	-	-	-	-	-	1
Growth rate[2]	0.54	0.47	0.53	0.43	0.53	0.34	0.38	0.36
DR[3]	12.4		5.0		7.6		2.4	

Fig. 7. Comparison of Pliar 53, *RhaRS/*P_{rhaB}, *XylS/*P_m and *LacI*^{q}/P_{trc} gene expression systems in *P. putida* KT2440. The activity, in terms of RFP fluorescence was measured in 96-well plates using growing cells at 30°C. The cultures were initiated at 0.2 OD_{600}. [1] Pi, rhamnose, m-toluic acid and IPTG Concentrations in mM. [2] Growth rate in h^{-1}. [3] Dynamic range, measured as the activity increase between the induced and repressed state.

Ready-to-use Pliar promoters synbio tool

Taken together, Pliar promoters have proved to be a very useful synbio tool to support automatic control of gene expression in biotechnological endeavours. In order to facilitate its portability and use by the community, we implemented several Pliar promoters in the context of the Standard European Vector Architecture, SEVA, platform (Martinez-Garcia *et al.*, 2019). SEVA is a synthetic biology platform aimed at assisting the choice of optimal genetic tools for de-constructing and re-constructing complex prokaryotic phenotypes. Since its launching, SEVA has become a widely used platform and its standards are well-known and largely accepted by the synbio community. Therefore, standardizing Pliar promoters within SEVA makes them available to a wide community of potential end users in a wide range of applications. Promoters displaying a high range of activity in *E. coli* and *P. putida* were selected to construct the ready-to-use tools. They included Pliar 53 (P*phoA*-like activity in both microorganisms); Pliar 15 (weak activity in both); Pliar 17 (medium strength in both); Pliar 51 (high strength in *E. coli* and medium strength in *P. putida*); Pliar 1 (low strength in *E. coli* and high strength in *P. putida*); and Pliar 70 (medium strength in *E. coli* and low strength in *P. putida*). Pliar promoters were

inserted between restriction sites *Pac*I and *Avr*II on the cargo site of a pSEVA231 vector, kanamycin resistant and with a broad range pBBR1 replication origin (Fig. S8). The final plasmids were named according to SEVA nomenclature: pSEVA2317 (Pliar 53); pSEVA2317A (Pliar 15); pSEVA2317B (Pliar 17); pSEVA2317C (Pliar 51); pSEVA2317D (Pliar 70); pSEVA2317E (Pliar 1). pSEVA2317 plasmids are available on the SEVA repository (http://seva-plasmids.com).

Conclusions

Synthetic biology largely aims to develop tools to speed up optimization of industrial processes. In this context, gene promoters play a major role because they are responsible for controlling gene transcription, thus providing the adequate protein load for target processes. In this work, we present a new set of nutrient-stress inducible promoters, the Pliar library. These new synthetic promoters are inspired by the PHO Pi-starvation system and were engineered by turning a strong constitutive promoter into a set of inducible promoters through the addition of PHO boxes at position −35. Pliar promoters increase the spectrum of activity strength from 0.4-fold to 1.3-fold compared to the wild-type P*phoA* and support fine control of biotechnological processes through selection of promoters that are best suited to the desired outputs.

Portability is one key aspect to consider when seeking and engineering new expression systems. Promoter portability supports the development of functional synbio tools in a large range of microorganisms. Extra regulatory elements are often required in the final constructs when developing these portable expression systems, which can entail subsequent increases in metabolic burdens in the host microorganism (Kushwaha and Salis, 2015). Due to the wide distribution of the PHO Pi-starvation system among bacteria (Fig. 1), synthetic Pliar promoters potentially represent a suitable tool to control gene expression in a large number of microorganisms without the need to introduce extra regulatory mechanisms. In this regard, the validation of the Pliar library in two biotechnological workhorses' microbial systems, *E. coli* W and *P. putida KT2440*, underpin potential portability of this system. In addition, SEVA-standardization of our library will facilitate future use of Pliar promoters in almost any bacterial strain with a functional PHO Pi-starvation system.

Widely used expression systems such as *Xyls/*P_m, *RhaRS/*P_{rhaB} and *LacI*^{q}/P_{trc} require expensive and/or toxic chemical inductors that limit their use in biotechnological applications. Furthermore, unlike Pliar promoters, they do not support the design of self-inducible biotechnological processes. Using *P. putida* KT2440 as a model, we proved here that Pliar promoters can be used to automatically induce any biotechnological process of interest. When using these promoters the reduction of extracellular Pi associated to bacterial growth and poly-Pi accumulation triggered a pre-programed Pi-starvation scenario, thus inducing the activation of the Pliar promoters without extra addition of chemical inductors. In addition, Pliar promoters are an interesting synbio tool for decoupling microbial growth from production, therefore avoiding the appearance of futile cycles and reducing metabolic burdens by simply adjusting phosphate concentrations in the fermentation medium.

Experimental procedures

The bacterial strains, plasmids and oligonucleotides used in this work are listed in Table 1.

For cloning, propagation and phosphate biosensor activity assays, *E. coli*, and *P. putida* strains were grown in LB medium or MOPS minimal medium (Neidhardt *et al.*, 1974) with 0.2% glucose as sole carbon source, with or without KH_2PO_4. Kanamycin (100 μg ml^{-1}) was added when necessary. *E. coli* were grown at 37°C and *P. putida* KT2440 at 30°C. Phosphate concentrations were calculated using Merck's phosphate assay kit and following the manufacturer's instructions.

DNA work

E. coli DH10B was used for cloning. DNA polymerases and other DNA modifying enzymes were purchased from New England Biolabs (Ipswich, MA, USA) and oligonucleotides were synthesized by Sigma-Aldrich (St. Louis, MO, USA). DNA purification kits were purchased from Nyztech (Lisboa, Portugal).

Construction of the PhoA-based phosphate biosensor

The *phoA* promoter from *E. coli* MG1655 was PCR-amplified and transcriptionally fused to the bicistronic translational coupler BCD2 (Mutalik *et al.*, 2013). The fluorescent *msfgfp* gene (GFP) from plasmid pBG42 (Zobel *et al.*, 2015) was used as reporter module. Subsequently, the P*phoA*::BCD2::*msfgfp* fragment was cloned using the *Pac*I/*Spe*I restriction sites in the broad host range pSEVA231 vector (Antoine and Locht, 1992; Martinez-Garcia *et al.*, 2019) and generating the pSEVA23_*phoA* vector Fig. 2A.

Construction of the synthetic phosphate promoters (Pliar) library

The PHO box logo sequence (Fig. 3A) was used as a template to design of a set of degenerated primers that

Table 1. Strains, plasmids and primers used in this work.

Strain	Phenotype	References
E. coli DH10B	F- mcrA Δ(mrr-hsdRMS-mcrBC) Φ80dlacZΔM15 ΔlacX74 endA1 recA1 deoR Δ(ara,leu)7697 araD139 galU galK nupG rpsL λ-	Grant *et al.* (1990)
E. coli W (ATCC 9637)	Wild-type strain	Archer *et al.* (2011)
P. putida KT2440	Wild-type strain	Bagdasarian *et al.* (1981)
Plasmid	Characteristics	ref
pBG42	Km^r, Gm^r, ori R6K, BCD2-*msfgfp*	Zobel *et al.* (2015)
pSEVA231	Km^r, ori pBBR1	Martinez-Garcia *et al.* (2019)
pSEVA234	Km^r, ori pBBR1, $LacI^q$/Ptrc	Martinez-Garcia *et al.* (2019)
pSEVA238	Km^r, ori pBBR1, XylS/Pm	Martinez-Garcia *et al.* (2019)
pSEVA237 M	Km^r, ori pBBR1, *msfgfp*	Martinez-Garcia *et al.* (2019)
E1010m (RFP)_CD	Ampr, ori pUC, *mrfp*1	Iverson et al. (2016)
pSEVA23_*phoA* (P*phoA*)	Km^r, ori pBBR1, P*phoA*-BCD2-*msfgfp*	This work
pSEVA23_BG42 (BG42)	Km^r, ori pBBR1, BG42-BCD2-*msfgfp*	This work
pSEVA23_Pliar 1 (Pliar 1)	Km^r, ori pBBR1, Pliar 1-BCD2-*msfgfp*	This work
pSEVA23_Pliar 10 (Pliar 10)	Km^r, ori pBBR1, Pliar 10-BCD2-*msfgfp*	This work
pSEVA23_Pliar 15 (Pliar 15)	Km^r, ori pBBR1, Pliar 15-BCD2-*msfgfp*	This work
pSEVA23_Pliar 17 (Pliar 17)	Km^r, ori pBBR1, Pliar 17-BCD2-*msfgfp*	This work
pSEVA23_Pliar 51 (Pliar 51)	Km^r, ori pBBR1, Pliar 51-BCD2-*msfgfp*	This work
pSEVA23_Pliar 52 (Pliar 52)	Km^r, ori pBBR1, Pliar 52-BCD2-*msfgfp*	This work
pSEVA23_Pliar 53 (Pliar 53)	Km^r, ori pBBR1, Pliar 53-BCD2-*msfgfp*	This work
pSEVA23_Pliar 59 (Pliar 59)	Km^r, ori pBBR1, Pliar 59-BCD2-*msfgfp*	This work
pSEVA23_Pliar 68 (Pliar 68)	Km^r, ori pBBR1, Pliar 68-BCD2-*msfgfp*	This work
pSEVA23_Pliar 70 (Pliar 70)	Km^r, ori pBBR1, Pliar 70-BCD2-*msfgfp*	This work
pSEVA2317	Km^r, ori pBBR1, Pliar 53	This work
pSEVA2317A	Km^r, ori pBBR1, Pliar 15	This work
pSEVA2317B	Km^r, ori pBBR1, Pliar 17	This work
pSEVA2317C	Km^r, ori pBBR1, Pliar 51	This work
pSEVA2317D	Km^r, ori pBBR1, Pliar 70	This work
pSEVA2317E	Km^r, ori pBBR1, Pliar 1	This work
pCMClv2_90	Gm^r, ori pBBR1, Pliar 53_*rfp*	This work
pCMClv2_91	Gm^r, ori pBBR1, *RhaRS/*P_{rhaB}*_rfp*	This work
pCMClv2_92	Gm^r, ori pBBR1, *XylS/*P_m*_rfp*	This work
pCMClv2_95	Gm^r, ori pBBR1, $LacI^q/P_{trc}$*_rfp*	This work
Primers	Sequence (5'-3')	ref
P*phoA*	GCGTTAATTAACAGCTGTCATAAAGTTGTCACGGCCGA GACTTATAGTCGCTTTGCCTAGGGCCCAAGTTCACTT AAAAAGGAGATC	This work
Pbg42	GCGTTAATTAAGCCCATTGACAAGGCTCTCGCG	This work
Pliar Degenerated primer	GCGTTAATTAAGNTKTMAYHWWHYNKTMAYCGCGGCC AGGTATAATTGCACGACCTAGGGCC	This work
PS2 (reverse Primer)	GCGGCAACCGAGCGTTC	Martinez-Garcia *et al.* (2019)
PS1 (sequencing primer)	AGGGCGGCGGATTTGTCC	Martinez-Garcia *et al.* (2019)

include randomized PHO Boxes (Table 1). These primers were used to construct the combinatorial library of synthetic Pliar promoters by PCR amplification. The constitutive promoter BG42 (5´-GCCCA**TTGACA**AGGCTCTCGCGGCCAGG**TATAAT**TGCACGA-3´) was used as a template. The structure of the synthetic promoters included promoter BG42's −10 region (5'-TATAAT-3') and a variable PHO box (5'-NTKTMAYHWWHYNKTMAY-3') located around the −35 region (Fig. 3 B). Figure 3C shows the strategy implemented to construct Pliar promoters.

Construction of the synthetic Pliar 53_rfp, RhaRS/P_{rhaB}*_rfp, XylS/*P_m*_rfp and* $LacI^q/P_{trc}$*_rfp expression systems*

The Codifying sequence for red fluorescence protein, RFP (E1010m (RFP)_CD) from the CIDAR Modular Cloning (MoClo) kit (Iverson *et al.*, 2016) was cloned using the SMOOTH MoClo developed in our lab (paper in preparation) under the control of the promoters Pliar 53, R*haRS/*P_{rhaB}, *XylS/*P_m and $LacI^q/P_{trc}$, generating the plasmids pCMClv2_90, pCMClv2_91, pCMClv2_92 and pCMClv2_95, respectively. The synthetic constructs were then introduced in *P. putida* KT2440 by electroporation.

Fluorescence-based promoter activity assay

The Pi depletion promoter activity assays were carried out as in Uluseker et al. (2019). Briefly, the *E. coli* and *P. putida* strains carrying the Pliar or P*phoA* were precultured overnight in MOPS minimal medium containing 5 mM KH_2PO_4 at 37°C and 30°C, respectively. Bacterial pre-cultures were used to inoculate the same fresh medium at 0.1 OD_{600} and were grown until mid-late exponential phase (0.6–0.9 OD_{600}). Bacterial cells were then

pelleted at 1500 *g*, room temperature for 10 min and washed twice in MOPS minimal medium without KH_2PO_4. For activity assays in cell-resting conditions, the bacteria were suspended at 2 OD_{600} in MOPS minimal medium 0.2% glucose, supplemented with Pi at the desired concentration. For activity assays in cell-growing conditions, bacterial cells were suspended at 0.2 OD_{600} in MOPS minimal medium 0.4% glucose, supplemented with Pi at 0.05, 0.5, 1, 1.5 or 2.5 mM. The Promoters activity was monitored using a Varioskan Flash spectral scanning multimode reader (Thermo Scientific, Waltham, Massachusetts, USA) using for GFP a $\lambda_{Excitation}$ 488 nm; $\lambda_{Emission}$ 509 nm, and for RFP a $\lambda_{Excitation}$ 580 nm; $\lambda_{Emission}$ 625 nm.

Pliar activity parameters analysis

Sigmoidal dose–response curves (Ang *et al*., 2013; D'Ambrosio and Jensen, 2017; Mannan *et al*., 2017) were adjusted to a Hill´s function, Eq. 1, to calculate activity parameters of *phoA* and the synthetic Pliar promoters.

$$f(x) = b + \frac{a-b}{1+10^{(\log\theta - x)\cdot K}}, \quad (1)$$

where $f(x)$ is promoter activity, given as GFP/OD_{600}; b is basal activity; a is peak activity, θ is IC_{50}; x is phosphate concentration and K is Hill's slope.

Acknowledgements

This work was supported by the European Union's Horizon 2020 Research and Innovation Programme under Grant Agreements no. 686585 (Liar) and 814650 (SynBio4Flav) and the Spanish Ministerio de Ciencia e Innovación through RobExplode project: PID2019-108458RB-I00" (AEI /10.13039/501100011033). The authors thanks Dr. Ozan Kahramanogullari and Darwin Carranza for their assistance in data analysis and the construction of some plasmids, respectively and to Clive A. Dove for critical reading of the manuscript.

Funding Information

This work was supported by the European Union's Horizon 2020 Research and Innovation Programme under Grant Agreements no. 686585 (Liar) and 814650 (SynBio4Flav) and the Spanish Ministerio de Ciencia e Innovación through RobExplode project: PID2019-108458RB-I00" (AEI /10.13039/501100011033).

Conflict of interest

The authors declare no conflict of interests.

References

Ang, J., Harris, E., Hussey, B.J., Kil, R., and McMillen, D.R. (2013) Tuning response curves for synthetic biology. *ACS Synth Biol* **2:** 547–567.

Antoine, R., and Locht, C. (1992) Isolation and molecular characterization of a novel broad-host-range plasmid from *Bordetella bronchiseptica* with sequence similarities to plasmids from gram-positive organisms. *Mol Microbiol* **6:** 1785–1799.

Archer, C.T., Kim, J.F., Jeong, H., Park, J.H., Vickers, C.E., Lee, S.Y., and Nielsen, L.K. (2011) The genome sequence of *E. coli* W (ATCC 9637): comparative genome analysis and an improved genome-scale reconstruction of *E. coli*. *BMC Genom* **12:** 9.

Bagdasarian, M., Lurz, R., Ruckert, B., Franklin, F.C., Bagdasarian, M.M., Frey, J., and Timmis, K.N. (1981) Specific-purpose plasmid cloning vectors. II. Broad host range, high copy number, RSF1010-derived vectors, and a host-vector system for gene cloning in Pseudomonas. *Gene* **16:** 237–247.

Blanco, A.G., Canals, A., and Coll, M. (2012) PhoB transcriptional activator binds hierarchically to pho box promoters. *Biol Chem* **393:** 1165–1171.

Blasi, B., Peca, L., Vass, I., and Kos, P.B. (2012) Characterization of stress responses of heavy metal and metalloid inducible promoters in synechocystis PCC6803. *J Microbiol Biotechnol* **22:** 166–169.

Bothfeld, W., Kapov, G., and Tyo, K.E.J. (2017) A glucose-sensing toggle switch for autonomous, high productivity genetic control. *ACS Synth Biol* **6:** 1296–1304.

Caspeta, L., Flores, N., Perez, N.O., Bolivar, F., and Ramirez, O.T. (2009) The effect of heating rate on *Escherichia coli* metabolism, physiological stress, transcriptional response, and production of temperature-induced recombinant protein: a scale-down study. *Biotechnol Bioeng* **102:** 468–482.

Ciccarelli, F.D., Doerks, T., von Mering, C., Creevey, C.J., Snel, B., and Bork, P. (2006) Toward automatic reconstruction of a highly resolved tree of life. *Science* **311:** 1283–1287.

Crooks, G.E., Hon, G., Chandonia, J.M., and Brenner, S.E. (2004) WebLogo: a sequence logo generator. *Genome Res* **14:** 1188–1190.

D'Ambrosio, V., and Jensen, M.K. (2017) Lighting up yeast cell factories by transcription factor-based biosensors. *FEMS Yeast Res* **17:** fox076.

de Lorenzo, V., Eltis, L., Kessler, B., and Timmis, K.N. (1993) Analysis of Pseudomonas gene products using lacIq/Ptrp-lac plasmids and transposons that confer conditional phenotypes. *Gene* **132:** 17–24.

Dollard, M.A., and Billard, P. (2003) Whole-cell bacterial sensors for the monitoring of phosphate bioavailability. *J Microbiol Methods* **55:** 221–229.

Durante-Rodriguez, G., de Lorenzo, V., and Nikel, P.I. (2018) A post-translational metabolic switch enables complete decoupling of bacterial growth from biopolymer production in engineered *Escherichia coli*. *ACS Synth Biol* **7:** 2686–2697.

Eisen, M.B., Spellman, P.T., Brown, P.O., and Botstein, D. (1998) Cluster analysis and display of genome-wide

expression patterns. *Proc Natl Acad Sci USA* **95:** 14863–14868.
Engstrom, M.D., and Pfleger, B.F. (2017) Transcription control engineering and applications in synthetic biology. *Synth Syst Biotechnol* **2:** 176–191.
Felpeto-Santero, C., Rojas, A., Tortajada, M., Galan, B., Ramon, D., and Garcia, J.L. (2015) Engineering alternative isobutanol production platforms. *AMB Express* **5:** 119.
Gao, R., and Stock, A.M. (2013) Evolutionary tuning of protein expression levels of a positively autoregulated two-component system. *PLoS Genet* **9:** e1003927.
Gao, R., and Stock, A.M. (2015) Temporal hierarchy of gene expression mediated by transcription factor binding affinity and activation dynamics. *MBio* **6:** e00686–e615.
Gao, R., and Stock, A.M. (2018) Overcoming the cost of positive autoregulation by accelerating the response with a coupled negative feedback. *Cell Rep* **24:** 3061–3071 e3066.
Gawin, A., Valla, S., and Brautaset, T. (2017) The XylS/Pm regulator/promoter system and its use in fundamental studies of bacterial gene expression, recombinant protein production and metabolic engineering. *Microbiol Biotechnol* **10:** 702–718.
Givskov, M., Eberl, L., Moller, S., Poulsen, L.K., and Molin, S. (1994) Responses to nutrient starvation in *Pseudomonas putida* KT2442: analysis of general cross-protection, cell shape, and macromolecular content. *J Bacteriol* **176:** 7–14.
Grant, S.G., Jessee, J., Bloom, F.R., and Hanahan, D. (1990) Differential plasmid rescue from transgenic mouse DNAs into *Escherichia coli* methylation-restriction mutants. *Proc Natl Acad Sci USA* **87:** 4645–4649.
Hicks, M., Bachmann, T.T., and Wang, B. (2020) Synthetic biology enables programmable cell-based biosensors. *ChemPhysChem* **21:** 132–144.
Hsieh, Y.J., and Wanner, B.L. (2010) Global regulation by the seven-component Pi signaling system. *Curr Opin Microbiol* **13:** 198–203.
Iverson, S.V., Haddock, T.L., Beal, J., and Densmore, D.M. (2016) CIDAR MoClo: improved MoClo assembly standard and new *E. coli* part library enable rapid combinatorial design for synthetic and traditional biology. *ACS Synth Biol* **5:** 99–103.
Jeske, M., and Altenbuchner, J. (2010) The *Escherichia coli* rhamnose promoter rhaP(BAD) is in *Pseudomonas putida* KT2440 independent of Crp-cAMP activation. *Appl Microbiol Biotechnol* **85:** 1923–1933.
Johnson, A.O., Gonzalez-Villanueva, M., Tee, K.L., and Wong, T.S. (2018) An engineered constitutive promoter set with broad activity range for *Cupriavidus necator* H16. *ACS Synth Biol* **7:** 1918–1928.
Kent, R., and Dixon, N. (2019) Contemporary tools for regulating gene expression in bacteria. *Trends Biotechnol* **38:** 316–333.
Kikuchi, Y., Yoda, K., Yamasaki, M., and Tamura, G. (1981) The nucleotide sequence of the promoter and the amino-terminal region of alkaline phosphatase structural gene (phoA) of *Escherichia coli*. *Nucleic Acids Res* **9:** 5671–5678.
Kulakovskaya, T. (2015) Phosphorus storage in microorganisms: diversity and evolutionary insight. *Biochem Physiol* **4:** 1000–1130.
Kushwaha, M., and Salis, H.M. (2015) A portable expression resource for engineering cross-species genetic circuits and pathways. *Nat Commun* **6:** 7832.
Lemmerer, M., Mairhofer, J., Lepak, A., Longus, K., Hahn, R., and Nidetzky, B. (2019) Decoupling of recombinant protein production from *Escherichia coli* cell growth enhances functional expression of plant Leloir glycosyltransferases. *Biotechnol Bioeng* **116:** 1259–1268.
Liu, M., Tolstorukov, M., Zhurkin, V., Garges, S., and Adhya, S. (2004) A mutant spacer sequence between -35 and -10 elements makes the Plac promoter hyperactive and cAMP receptor protein-independent. *Proc Natl Acad Sci USA* **101:** 6911–6916.
Lo, T.M., Chng, S.H., Teo, W.S., Cho, H.S., and Chang, M.W. (2016) A two-layer gene circuit for decoupling cell growth from metabolite production. *Cell Syst* **3:** 133–143.
Lübke, C., Boidol, W., and Petri, T. (1995) Analysis and optimization of recombinant protein production in *Escherichia coli* using the inducible pho A promoter of the *E. coli* alkaline phosphatase. *Enzyme Microbial Technol* **17:** 923–928.
Mannan, A.A., Liu, D., Zhang, F., and Oyarzun, D.A. (2017) Fundamental design principles for transcription-factor-based metabolite biosensors. *ACS Synth Biol* **6:** 1851–1859.
Martinez-Garcia, E., Goni-Moreno, A., Bartley, B., McLaughlin, J., Sanchez-Sampedro, L., Pascual Del Pozo, H., *et al*. (2019) SEVA 3.0: an update of the Standard European Vector Architecture for enabling portability of genetic constructs among diverse bacterial hosts. *Nucleic Acids Res* **48:** 3395.
Menart, V., Jevsevar, S., Vilar, M., Trobis, A., and Pavko, A. (2003) Constitutive versus thermoinducible expression of heterologous proteins in *Escherichia coli* based on strong PR, PL promoters from phage lambda. *Biotechnol Bioeng* **83:** 181–190.
Miyake, T., Oka, T., Nishizawa, T., Misoka, F., Fuwa, T., Yoda, K., *et al*. (1985) Secretion of human interferon-alpha induced by using secretion vectors containing a promoter and signal sequence of alkaline phosphatase gene of *Escherichia coli*. *J Biochem* **97:** 1429–1436.
Mutalik, V.K., Guimaraes, J.C., Cambray, G., Lam, C., Christoffersen, M.J., Mai, Q.A., *et al*. (2013) Precise and reliable gene expression via standard transcription and translation initiation elements. *Nat Methods* **10:** 354–360.
Neidhardt, F.C., Bloch, P.L., and Smith, D.F. (1974) Culture medium for enterobacteria. *J Bacteriol* **119:** 736–747.
Nesmeyanova, M.A. (2000) Polyphosphates and enzymes of polyphosphate metabolism in *Escherichia coli*. *Biochemistry (Mosc)* **65:** 309–314.
Nevoigt, E., Fischer, C., Mucha, O., Matthaus, F., Stahl, U., and Stephanopoulos, G. (2007) Engineering promoter regulation. *Biotechnol Bioeng* **96:** 550–558.
Nikel, P.I., Chavarria, M., Martinez-Garcia, E., Taylor, A.C., and de Lorenzo, V. (2013) Accumulation of inorganic polyphosphate enables stress endurance and catalytic vigour in *Pseudomonas putida* KT2440. *Microb Cell Fact* **12:** 50.

Nikel, P.I., and de Lorenzo, V. (2018) Pseudomonas putida as a functional chassis for industrial biocatalysis: from native biochemistry to trans-metabolism. *Metab Eng* **50:** 142–155.

Palomares, L.A., Estrada-Mondaca, S., and Ramirez, O.T. (2004) Production of recombinant proteins: challenges and solutions. *Methods Mol Biol* **267:** 15–52.

Park, J.H., Jang, Y.S., Lee, J.W., and Lee, S.Y. (2011) *Escherichia coli* W as a new platform strain for the enhanced production of L-valine by systems metabolic engineering. *Biotechnol Bioeng* **108:** 1140–1147.

Poblete-Castro, I., Becker, J., Dohnt, K., dos Santos, V.M., and Wittmann, C. (2012) Industrial biotechnology of *Pseudomonas putida* and related species. *Appl Microbiol Biotechnol* **93:** 2279–2290.

Qing, G., Ma, L.C., Khorchid, A., Swapna, G.V., Mal, T.K., Takayama, M.M., *et al*. (2004) Cold-shock induced high-yield protein production in *Escherichia coli*. *Nat Biotechnol* **22:** 877–882.

Ritzefeld, M., Walhorn, V., Kleineberg, C., Bieker, A., Kock, K., Herrmann, C., *et al*. (2013) Cooperative binding of PhoB(DBD) to its cognate DNA sequence-a combined application of single-molecule and ensemble methods. *Biochemistry* **52:** 8177–8186.

Sanders, J.W., Venema, G., Kok, J., and Leenhouts, K. (1998) Identification of a sodium chloride-regulated promoter in *Lactococcus lactis* by single-copy chromosomal fusion with a reporter gene. *Mol Gen Genet* **257:** 681–685.

Santos-Beneit, F. (2015) The Pho regulon: a huge regulatory network in bacteria. *Front Microbiol* **6:** 402.

Schneider, T.D., and Stephens, R.M. (1990) Sequence logos: a new way to display consensus sequences. *Nucleic Acids Res* **18:** 6097–6100.

Soma, Y., and Hanai, T. (2015) Self-induced metabolic state switching by a tunable cell density sensor for microbial isopropanol production. *Metab Eng* **30:** 7–15.

Stargardt, P., Feuchtenhofer, L., Cserjan-Puschmann, M., Striedner, G., and Mairhofer, J. (2020) Bacteriophage inspired growth-decoupled recombinant protein production in *Escherichia coli*. *ACS Synth Biol* **9:** 1336–1348.

Uluseker, C., Torres-Bacete, J., Garcia, J.L., Hanczyc, M.M., Nogales, J., and Kahramanogullari, O. (2019) Quantifying dynamic mechanisms of auto-regulation in *Escherichia coli* with synthetic promoter in response to varying external phosphate levels. *Sci Rep* **9:** 2076.

Valdez-Cruz, N.A., Caspeta, L., Perez, N.O., Ramirez, O.T., and Trujillo-Roldan, M.A. (2010) Production of recombinant proteins in *E. coli* by the heat inducible expression system based on the phage lambda pL and/or pR promoters. *Microb Cell Fact* **9:** 18.

Van Dien, S.J., and Keasling, J.D. (1998) A dynamic model of the *Escherichia coli* phosphate-starvation response. *J Theor Biol* **190:** 37–49.

Vasquez, J.R., Evnin, L.B., Higaki, J.N., and Craik, C.S. (1989) An expression system for trypsin. *J Cell Biochem* **39:** 265–276.

von der Heyde, E.L., Klein, B., Abram, L., and Hallmann, A. (2015) The inducible nitA promoter provides a powerful molecular switch for transgene expression in *Volvox carteri*. *BMC Biotechnol* **15:** 5.

Yang, S., Liu, Q., Zhang, Y., Du, G., Chen, J., and Kang, Z. (2018) Construction and characterization of broad-spectrum promoters for synthetic biology. *ACS Synth Biol* **7:** 287–291.

Yin, J., Li, G., Ren, X., and Herrler, G. (2007) Select what you need: a comparative evaluation of the advantages and limitations of frequently used expression systems for foreign genes. *J Biotechnol* **127:** 335–347.

Zobel, S., Benedetti, I., Eisenbach, L., de Lorenzo, V., Wierckx, N., and Blank, L.M. (2015) Tn7-based device for calibrated heterologous gene expression in *Pseudomonas putida*. *ACS Synth Biol* **4:** 1341–1351.

Supporting information

Additional supporting information may be found online in the Supporting Information section at the end of the article.

Fig. S1. Sequence alignment of PHO boxes from diverse sources and PHO box consensus sequence used for the design of degenerated primers.

Fig. S2. Time course of P*phoA* activity at limited (50 μM) and plenty (1 mM) phosphate concentration in *E. coli* W (A) and *P. putida* KT2440 (B). P*phoA* activity was measured as GFP expression in MOPS minimal medium with 0.2% glucose supplemented with phosphate at 37 C for *E. coli* and 30 C for *P. putida*.

Fig. S3. Time course of P*phoA* and Pliar promoters' activity over the time in *E. coli* W in resting cells at increasing phosphate concentrations. Promoters' activity was measured as GFP expression in MOPS minimal medium with 0.2% glucose at 37°C.

Fig. S4. Dose–response curves (Hill´s function) of synthetic Pliar promoters in *E. coli* W resting cells after 3.5 h' incubation. Activity was measured as GFP expression and normalized considering P*phoA*'s peak activity as the reference (value of 1) in MOPS minimal medium with 0.2% glucose at 37°C.

Fig. S5. Time course of P*phoA* and Pliar promoters' activity in *P. putida* KT2440 resting cells at increasing phosphate concentrations. Promoters' activity was measured as GFP expression in MOPS minimal medium with 0.2% glucose at 30°C.

Fig. S6. Dose–response curves (Hill´s function) of synthetic Pliar promoters in *P. putida* KT2440 resting cells after 3.5 h' incubation. Activity was measured as GFP expression and normalized considering P*phoA*'s peak activity as the reference (value of 1) in MOPS minimal medium with 0.2% glucose at 30°C.

Fig. S7. Time course of growth and activity of the Pliar 53, $RhaRS/P_{rhaB}$, $XylS/P_m$ and $LacI^q/P_{trc}$ promoter systems in *P. putida* KT2440. The activity in terms of RFP fluorescence was measured in 96-well plates using growing cells at 30°C in MOPS minimal medium 0.4% glucose, supplemented with 5 mM Pi. The cultures were initiated at 0.2 OD_{600}. For induction, the cells carrying the Pliar 53 promoter were grown at 0.5 mM Pi; cells carrying $RhaRS/P_{rhaB}$ were grown at 1 mM rhamnose; cells carrying $XylS/P_m$ were grown at 1 mM m-toluic acid and cells carrying the $LacI^q/P_{trc}$ promoter system were grown at 1 mM IPTG.

Fig. S8. Up, Schematic structure map of pSEVA1317 vectors. The position of the Pliar promoter is highlighted in dark green. KmR (kanamycin resistant). oriT is highlighted in purple and the origin of replication pBBR1 in blue. Down, nucleotide sequence of the Pliar promoters selected: pSEVA2317 (Pliar 53); pSEVA2317A (Pliar 15); pSEVA2317B (Pliar 17); pSEVA2317C (Pliar 51); pSEVA2317D (Pliar 70); pSEVA2317E (Pliar 1). Underline the sequence of the restriction enzymes *Pac*I and *Avr*II.

